



Article

Evaluation of UV-C Radiation Efficiency in the Decontamination of Inanimate Surfaces and Personal Protective Equipment Contaminated with Phage $\phi 6$

Maria Bartolomeu [†], Márcia Braz [†], Pedro Costa [†], João Duarte [†], Carla Pereira ^{*} and Adelaide Almeida ^{*}

Department of Biology and CESAM, Campus Universitário de Santiago, University of Aveiro, 3810-193 Aveiro, Portugal; maria.bartolomeu@ua.pt (M.B.); marciabraz96@ua.pt (M.B.);

pedrommrcosta@ua.pt (P.C.); j.macedoduarte@ua.pt (J.D.)

* Correspondence: csgp@ua.pt (C.P.); aalmeida@ua.pt (A.A.)

[†] These authors contributed equally to this work.

Abstract: To help halt the global spread of the severe acute respiratory syndrome coronavirus 2 (SARS-CoV-2), appropriate disinfection techniques are required. Over the last years, the interest in Ultraviolet-C (UV-C) radiation as a method to disinfect inanimate surfaces and personal protective equipment (PPE) has increased, mainly to efficiently disinfect and prevent SARS-CoV-2 from spreading and allow for the safe reuse of said equipment. The bacteriophage $\phi 6$ (or simply phage $\phi 6$) is an RNA virus with a phospholipid envelope and is commonly used in environmental studies as a surrogate for human RNA-enveloped viruses, including SARS-CoV-2. The present study investigated the use of two new UV irradiation systems ((2)2.4W and (8)5.5W) constituted by conventional mercury UV-C lamps with a strong emission peak at ~254 nm to potentially inactivate phage $\phi 6$ on different surfaces (glass, plastic, stainless steel, and wood) and personal protective equipment, PPE, (surgical and filtering facepiece 2, FFP2, masks, a clear acetate visor, and disposable protective clothing). The results showed that both UV-C systems were effective in inactivating phage $\phi 6$, but the UV-C sterilizing chamber (8)5.5W had the best disinfection performance on the tested surfaces. The inactivation effectiveness is material-dependent on all surfaces, reaching the detection limit of the method at different times (between 60 and 240 s of irradiation). The glass surface needed less time to reduce the virus (30 s) when compared with plastic, stainless, and wood surfaces (60 s). The virus inactivation was more effective in the disposable surgical and FFP2 masks (60 and 120 s, respectively) than in the disposable vest and clear acetate visor (240 s). Overall, this study suggests that UV-C lamps with peak emission at ~254 nm could provide rapid, efficient, and sustainable sanitization procedures to different materials and surfaces. However, dosage and irradiation time are important parameters to be considered during their implementation as a tool in the fight against human coronaviruses, namely against SARS-CoV-2.

Keywords: SARS-CoV-2 surrogate; phage $\phi 6$; UV-C light; disinfection; surfaces; personal protective equipment



Citation: Bartolomeu, M.; Braz, M.; Costa, P.; Duarte, J.; Pereira, C.; Almeida, A. Evaluation of UV-C Radiation Efficiency in the Decontamination of Inanimate Surfaces and Personal Protective Equipment Contaminated with Phage $\phi 6$. *Microorganisms* **2022**, *10*, 593. <https://doi.org/10.3390/microorganisms10030593>

Academic Editor: Garima Sharma

Received: 14 February 2022

Accepted: 7 March 2022

Published: 9 March 2022

Publisher's Note: MDPI stays neutral with regard to jurisdictional claims in published maps and institutional affiliations.



Copyright: © 2022 by the authors. Licensee MDPI, Basel, Switzerland. This article is an open access article distributed under the terms and conditions of the Creative Commons Attribution (CC BY) license (<https://creativecommons.org/licenses/by/4.0/>).

1. Introduction

The COVID-19 pandemic disease caused by the SARS-CoV-2 is a serious health problem worldwide [1]. The respiratory virus SARS-CoV-2 is shed in high concentrations in respiratory secretions and is mainly transmitted through respiratory droplets and close contact with infected people [2]. Furthermore, this virus can also spread through nasal, oral, and ocular mucus-contaminated surfaces [3]. The importance of contaminated surfaces and fomites in the transmission is uncertain [4]. However, some studies have demonstrated that SARS-CoV-2 can survive on static surfaces such as metal, glass, or plastic for several days [5,6]. Chin et al. (2020) found that it remained viable for up to 1 day on cloth and wood, up to 2 days on glass, 4 days on stainless steel and plastic, and up to 7 days on

the outer layer of a medical mask [5]. Another study found that the virus survived 4 h on copper, 24 h on cardboard, and up to 72 h on plastic and stainless steel [6]. Gidari et al. (2021) observed that SARS-CoV-2 remained viable on plastic and glass for 120 h and stainless steel for 72 h [7]. In fact, Gonçalves et al. (2021) reported that the highest rate of SARS-CoV-2 was found in COVID-19 isolation wards, followed by a single study in a diagnostic laboratory, public transport systems, and long-term care facilities [8]. Recently, Kampf et al. (2020) observed that the detection rate of SARS-CoV was variable on inanimate surfaces (0–75%) of intensive care units, in isolation rooms (1.4–100%), and in general wards (0–61%) [9]. The coronavirus concentrations per swab were 4.4–5.2 log₁₀ on intensive care units and 2.8–4.0 log₁₀ on general wards [10]. In another study, Lv et al. (2020) reported that the materials/surfaces with the highest density of SARS-CoV-2 nucleic acid were outer gloves (37.4 copies/cm²), followed by door handles (26.25 copies/cm²), goggles (22.16 copies/cm²), and the outer cover and the inner wall of a high-speed centrifuge (19.95 and 14.70 copies/cm², respectively) [11]. The level of contamination on surfaces and PPE is influenced by several factors that include the status of COVID-19 patients in the vicinity of the sampling areas, cleaning and disinfection, environmental factors (such as temperature, pH, and humidity), sampling procedures, and detection methods [5,8,12–15].

With the rapid increase in COVID-19 cases worldwide, strategies were implemented to limit the spread of SARS-CoV-2, including increased use of PPE and cleaning and disinfection procedures [16]. Such procedures may include heat sterilization, chemical disinfectants, filtration, and UV irradiation [1,7]. However, UV radiation disinfection is the one that offers the most advantages because it can be performed automatically and can be employed to efficiently control microbial growth in any medium and disinfect surfaces, liquids, air, and rooms; it is also very energy efficient [1,16]. In particular, UV-C light at wavelengths of approximately 254 nm exerts bactericidal and virucidal effects, and it is widely used to disinfect enclosed spaces [17].

UV light can directly affect viruses by modifying their genetic material (either DNA or RNA) and/or damaging their proteins/lipids, but inactivation is dominated by nucleic acid damage [1,18,19]. Absorbed UV-C light damages the virus nucleic acid, inducing the photochemical fusion of two adjacent pyrimidines into covalent-linked dimers, namely uracil/cytosine dimers in RNA and thymine/cytosine dimers in DNA [1,18,19]. Other mechanisms of UV-light inactivation include RNA-protein cross-linking [20] and site-specific damage to RNA or proteins through energy transfer between the two molecules [21]. This then leads to the cell's inability to replicate and jeopardises its survival [1,22]. Nonetheless, each microbe has a different susceptibility to the UV wavelength and this will alter the effectiveness of the UV disinfection mechanism [1]. This susceptibility varies widely with the type of nucleic acids (DNA or RNA) and, as it happens in most viruses, with its genome structure (single- or double-stranded) [23]. Since lethal UV irradiation photoproducts are commonly thymine dimers, RNA viruses, such as the SARS-CoV-2 virus, are more resistant to UV radiation damage than DNA viruses [24,25]. However, capsid proteins, which protect the nucleic acids [26,27], are also easily disrupted (degraded and aggregated) by UV irradiation, leading to structural changes in the virus, impacting the virus's ability to infect [28]. UV exposure also causes an increase in methyl groups associated with lipids, lipid oxidation, and also leads to alterations in lipid composition of viral lipidic envelopes [29] present in enveloped viruses, such as in the SARS-CoV-2 virus, surrounding the protein capsid. This makes the SARS-CoV-2 highly susceptible to UV-C irradiation and, as different studies have demonstrated, can lead to its rapid inactivation on surfaces and supplies [30–34]. The UV-C irradiation efficacy is substantially reduced by the increasing distance between the light source and the target, the surface's matrix, and light reflection and scattering [35,36]. Therefore, the ideal fomites for UV-C decontamination should be non-porous and smooth, allowing them to be placed under the bulbs for short exposure cycles [36].

This study aimed to evaluate the efficiency of two UV irradiation systems on inanimate surfaces (plastic, glass, stainless steel, and wood and PPE (surgical and FFP2

masks, clear acetate visor, and disposable protective clothing)) contaminated with phage $\Phi 6$, used as SARS-CoV-2 surrogate, as additional help in the fight against the COVID-19 pandemic. Given the difficulty (pathogenicity, genetic mutations frequency, biosafety level 3/4) in working with highly infectious human viruses, namely coronaviruses, many researchers have considered the potential of phages, viruses that only infect bacteria, as models to measure the survival, transfer, and removal of human viruses [37–39]. Phage $\phi 6$ is an enveloped RNA virus that has been suggested as a good surrogate for the study of enveloped RNA viruses [40–43] such as SARS-CoV-2 [44]. Similar to SARS-CoV-2, phage $\phi 6$ has a lipid membrane, spike proteins, similar size (~80–100 nm) [44] and has an RNA genome (SARS-CoV-2 is a non-segmented single-stranded positive-sense RNA, with a length of ~30 kb [45] and phage $\phi 6$ is a three-part, segmented, double-stranded RNA genome, with ~13.5 kb in length [46]).

2. Materials and Methods

2.1. Bacterial Strain and Growth Conditions

Phage $\phi 6$ bacterial host strain, *Pseudomonas syringae* pv. *syringae* (DSM 21482), was acquired from Leibniz-Institute DSMZ—Deutsche Sammlung von Mikroorganismen und Zellkulturen GmmH (Braunschweig, Germany) [47]. The bacterial strain was stored at $-80\text{ }^{\circ}\text{C}$ in 10% glycerol. Before each assay, a stock culture of the bacteria was aseptically inoculated in 30 mL of Tryptic Soy Broth (TSB; Liofilchem, Roseto degli Abruzzi, Italy) and was grown for 18 h at $25\text{ }^{\circ}\text{C}$ at 120 rpm stirring. An aliquot (300 μL) of this bacterial culture was transferred into a new fresh TSB medium and grown overnight at $25\text{ }^{\circ}\text{C}$ to reach an absorbance at 600 nm of 0.8 (HaloDB-20; DynamicaScientific, Livingston, UK), corresponding approximately to 10^9 cells per mL.

2.2. Preparation of Virus Suspension

Phage $\phi 6$ (DSM 21518) was used in this study as a model of SARS-CoV-2 and was acquired from Leibniz-Institute DSMZ—Deutsche Sammlung von Mikroorganismen und Zellkulturen GmmH (Braunschweig, Germany) [47]. Phage $\phi 6$ is an RNA phage that belongs to the *Cystoviridae* family [48,49]. Phage suspensions were prepared from a phage stock previously prepared in SM buffer [0.1 M NaCl (Sigma, St. Louis, MO, USA), 8 mM MgSO_4 (Sigma, St. Louis, MO, USA), 20 mM Tris-HCl (Sigma, St. Louis, MO, USA), 2% (*w/v*) gelatin, pH 7.5] using *P. syringae* pv. *syringae* as the host and according to a previous study of our research group [47]. The phage suspension was stored at $4\text{ }^{\circ}\text{C}$ until use and the titer was determined through the double-layer agar method [50]. Successive dilutions of the phage suspension were performed in phosphate-buffered saline [PBS; 137 mM NaCl (Sigma, St. Louis, MO, USA), 2.7 mM KCl (Sigma, St. Louis, MO, USA), 8.1 mM $\text{Na}_2\text{HPO}_4 \cdot 2\text{H}_2\text{O}$, 1.76 mM KH_2PO_4 (Sigma, St. Louis, MO, USA), pH 7.4], and 500 μL of each dilution was added to 200 μL of fresh *P. syringae* pv. *syringae* culture, mixed with 5 mL of TSB 0.6% top agar layer [30 g/L TSB (Liofilchem, Roseto degli Abruzzi, Italy), 6 g/L agar (Liofilchem, Roseto degli Abruzzi, Italy), 0.05 g/L CaCl_2 (Sigma, St. Louis, MO, USA), 0.12 g/L MgSO_4 (Sigma, St. Louis, MO, USA), pH 7.4] and poured over a Tryptic Soy Agar (TSA; Liofilchem, Roseto degli Abruzzi, Italy) plate. The plates were incubated at $25\text{ }^{\circ}\text{C}$ for 18 h and the results were expressed as plaque-forming units per millilitre (PFU/mL).

2.3. UV-C Light System, Lamps Characteristics, and Irradiation Systems

The UV-C sterilizing chamber (2)2.4W (Climar lighting) included two compact fluorescent germicidal UV-C lamps [9 W nominal power, 2-pin G23 base, twin-tube lamp with dimensions of 14.5 cm length and 2.8 cm diameter, operating on 120–277 V AC @ 50/60 Hz, (FRL-6-1X-G23-9W-UVC, Larson Electronics, Kemp, TX, USA)] providing a 2.4W UV-C output at a UV wavelength of 253.7 nm (Figure 1a). The UV-C lamps have low mercury content, are long-lasting due to the specific coating, and are ozone-free. The samples were

placed approximately 20 cm from the two lamps (Figure 1a), with an average irradiance between 1.0–2.5 mW/cm².

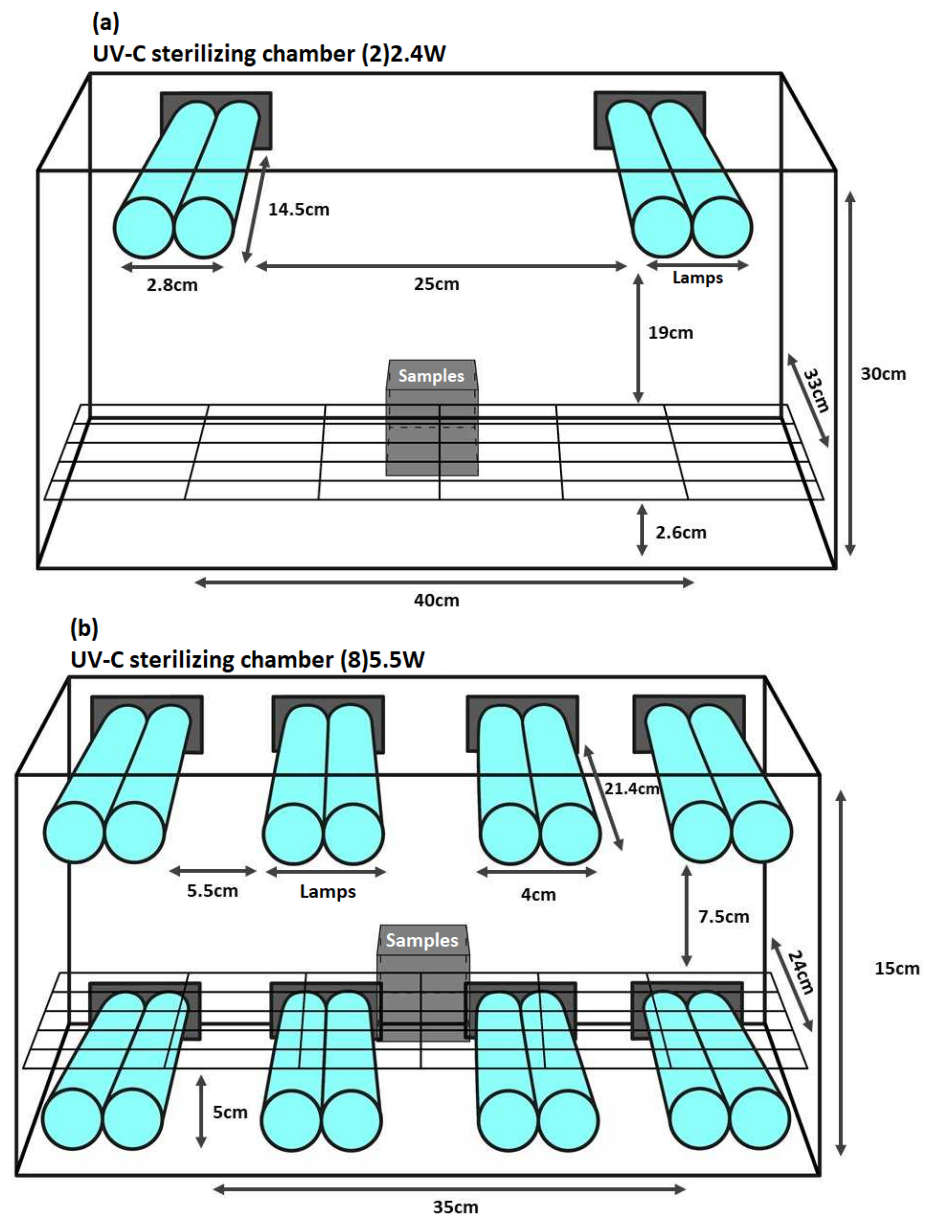


Figure 1. UV-C light disinfection systems. (a) UV-C sterilizing chamber (2)2.4W; the samples were placed approximately 20 cm from the two lamps and (b) UV-C sterilizing chamber (8)5.5W; the samples were placed approximately 7 cm from the top four lamps and approximately 2 cm from the bottom four lamps.

The UV-C sterilizing chamber (8)5.5W light disinfection system included eight UV-C germicidal lamps [18 W nominal power, 2G11 base, 21.4 cm length and 4.0 cm diameter, 58 V (Puritec HNS L 18 W 2G11, Osram, Garching, Germany)] providing a 5.5W UV-C output between 200–280 nm and a prevalent wavelength of 254 nm. The UV-C lamps have low mercury content, are long-lasting due to the specific coating, and are ozone-free. The samples were placed approximately 7 cm from the top four lamps and approximately 2 cm from the bottom four lamps (Figure 1b), with an average irradiance of 4.0 mW/cm².

The average irradiance at samples' level was measured with a laser power and energy meter FieldMaxII-TOP combined with a high-sensitivity thermopile sensor PS19Q (Coherent, Santa Clara, CA, USA).

The interior walls of both systems are lined with aluminium sheets, a highly reflective material.

2.4. Inanimate Surfaces and Personal Protective Equipment Preparation

The inanimate surfaces selected were plastic (polystyrene Petri dishes were used, Ø 90 mm, A = 63.60 cm²), glass (borosilicate Petri dishes were used, Ø 90 mm, A = 63.60 cm²), metal (stainless steel 304 L, A = 18.75 cm²), and wood (white-melamine faced chipboard sheets, A = 9.61 cm²). All materials were sterilized before use: polystyrene Petri dishes were purchased already sterilized by gamma rays; borosilicate Petri dishes and stainless-steel cuts were sterilized by autoclave; and wood pieces were disinfected with ethanol (70%) and sterilized with prolonged UV-C cycles of 2 min.

The PPE used in this work were surgical and FFP2 masks, clear acetate visor, and medical disposable protective clothing. Before each test, the PPE materials were cut into pieces (A = 6.0 cm² to surgical and FFP2 masks, and medical disposable protective clothing; A = 63.60 cm² to clear acetate visor). The PPE materials were sterilized before use by UV radiation for 2 min. After sterilization, the PPE pieces were aseptically placed in sterile Petri dishes.

2.5. UV-C Irradiation Assays

Inanimate surfaces and PPE were artificially contaminated with phage $\phi 6$ at a concentration of approximately 10⁸ PFU/mL. Surfaces and PPE were inoculated with ten droplets containing 10 μ L of the prepared inoculum, which retained their shape. Surfaces and PPE were exposed to UV-C radiation while the inoculum was still wet. Surfaces (glass, plastic, stainless steel, and wood) were exposed to both UV-C sterilizing systems. The PPE materials were only exposed to the UV-C sterilizing chamber (8)5.5W (selected according to the results of the tests on surfaces). Non-irradiated controls were also included in the different experiments. After exposure, aliquots of the surface test samples and controls were collected in 1 mL of PBS at time 0 and after 30, 60, and 120 s of irradiation. For the PPE, aliquots were collected at time 0 and after 30, 60, 120, 180, 240, 300, and 360 s of irradiation. Successive dilutions of the treated samples and controls were performed in sterile PBS and plated by the drop-plate method (5 μ L) in double-layered agar plates [50]. The plates were incubated at 25 °C for 12 h. The results were expressed in log PFU/mL as a function of irradiation time, in seconds. The detection limit of this method was 200 PFU/mL. Three independent experiments were performed for each condition and in each trial, three replicates were included.

2.6. Statistical Analysis

Statistical analysis of the data was performed using the GraphPad Prism 7.04 software (San Diego, CA, USA). After verifying the normal distribution of the data, the significance of viral concentrations between treatments, and throughout the trials, were evaluated by two-way ANOVA variance analysis. Tukey's multiple comparison test was used for pairwise comparison of means. For different treatments, the significance of the differences was evaluated by comparing the results obtained in the test samples with each other and with the results obtained in the controls, for different times. A *p*-value < 0.05 was considered significant. Three independent experiments with three replicates for each were performed.

3. Results

3.1. UV-C Irradiation Assays

3.1.1. Inanimate Surfaces

In the phage inactivation assays, it was observed that the UV-C sterilizing chamber (8)5.5W system inactivated the phage faster than the UV-C sterilizing chamber (2)2.4W. In both irradiation systems, differences were observed in the viral inactivation rate between each inanimate surface tested (Figures 2 and 3). In all experiments (Figures 2 and 3), the controls remained stable throughout the assay.

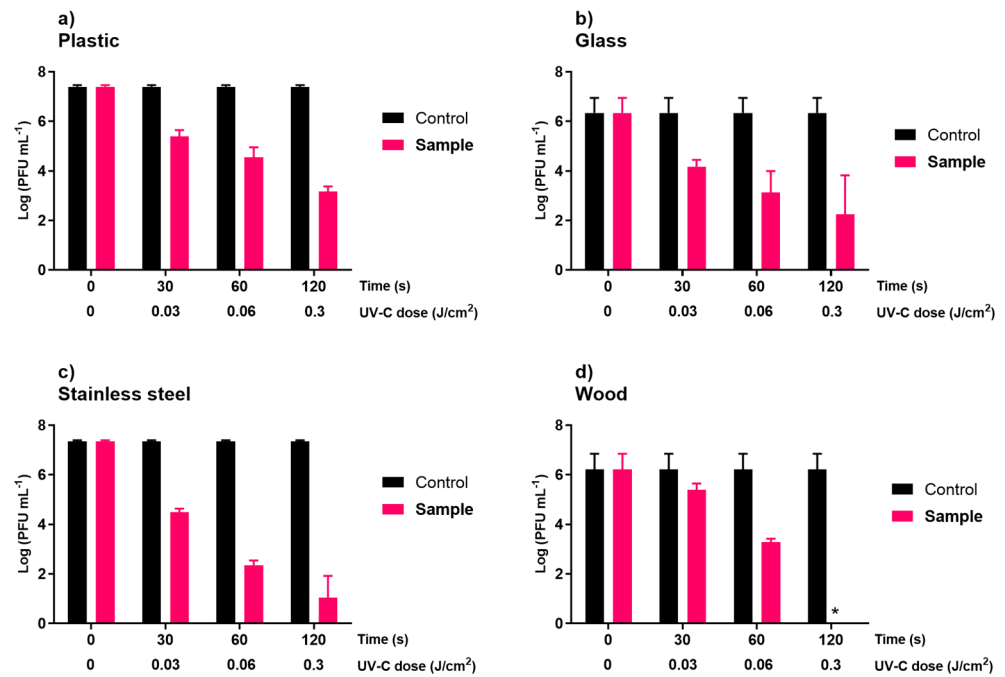


Figure 2. Inactivation of phage $\phi 6$ by the UV-C sterilizing chamber (2)2.4W on inanimate surfaces: plastic (a), glass (b), stainless steel (c), and wood (d). Limit of detection was about 2.3 log PFU/mL. Values represent the mean of the three experiments and error bars represent the standard deviation. * below the methods' detection limit.

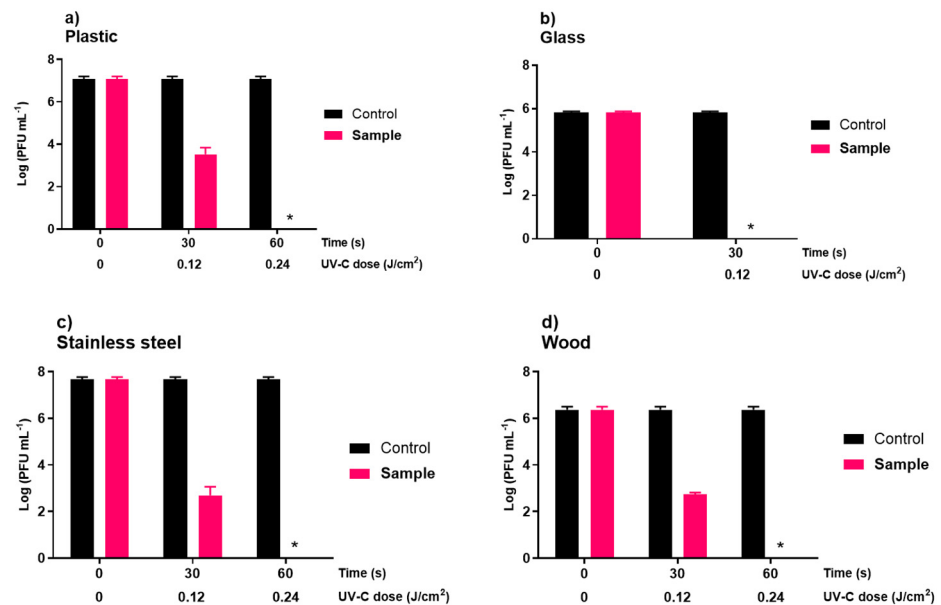


Figure 3. Inactivation of phage $\phi 6$ by the UV-C sterilizing chamber (8)5.5W on inanimate surfaces: plastic (a), glass (b), stainless steel (c), and wood (d). Limit of detection was about 2.3 log PFU/mL. Values represent the mean of the three experiments and error bars represent the standard deviation. * below the methods' detection limit.

In the UV-C sterilizing chamber (2)2.4W, the maximum viral inactivation was 4.1, 4.2, 6.3, and 6.2 log PFU/mL (ANOVA, $p < 0.05$) in plastic, glass, stainless steel, and wood, respectively, achieved after 120 s of irradiation (Figure 2). However, in plastic, after 30 and 60 s of irradiation, the viral inactivation was already 2.0 and 2.9 log PFU/mL (ANOVA, $p < 0.05$, Figure 2a). These results were similar (ANOVA, $p > 0.05$) to those observed in glass, with a 2.2 and 3.2 log PFU/mL decrease after 30 and 60 s of irradiation, respectively

(Figure 2b). In general, the viral inactivation in stainless steel (decrease 2.9, 5.0, and 6.3 log PFU/mL after 30, 60, and 120 s of irradiation, respectively; Figure 2c) was higher than that observed in glass, plastic, and wood. In wood (Figure 2d), the maximum rate of inactivation was similar (ANOVA, $p > 0.05$) to that obtained for the stainless steel after 120 s of irradiation. However, after 30 and 60 s of irradiation, the viral inactivation for wood (decrease 0.8 and 2.9 log PFU/mL after 30 and 60 s, respectively) was lower (ANOVA, $p < 0.05$, Figure 2c,d) than that observed in stainless steel.

The UV-C sterilizing chamber (8)5.5W was able to inactivate phage $\phi 6$ below the detection limit of the method in all inanimate surfaces tested. In plastic, the detection limit of the method (inactivation of 7.1 log PFU/mL) was reached after 60 s (Figure 3a). However, the viral concentration decreased by approximately 3.6 log PFU/mL (ANOVA, $p < 0.05$, Figure 3a) after 30 s of irradiation. When the glass was disinfected with the UV-C light disinfection system, a reduction of approximately 6.0 log PFU/mL (ANOVA, $p < 0.05$, Figure 3b) was observed just after 30 s of irradiation, reaching the detection limit of the method. In stainless steel plates (Figure 3c), the inactivation reached the detection limit (7.7 log PFU/mL) after 60 s of irradiation (with 5.0 log PFU/mL decrease after just 30 s of irradiation). In wood (Figure 3d), a 3.7 log PFU/mL inactivation was achieved after 30 s, and the detection limit of the method was reached after 60 s of irradiation (6.4 log PFU/mL decrease).

3.1.2. Personal Protective Equipment

In the UV-C sterilizing chamber (8)5.5W, viral inactivation was demonstrated to be material-dependent; the detection limit of the method was reached after 60, 120, 240, and 240 s of irradiation for disposable surgical masks, FFP2 masks, clear acetate visors, and disposable protective vests, respectively. In all assays (Figure 4), the controls remained constant throughout the experiment.

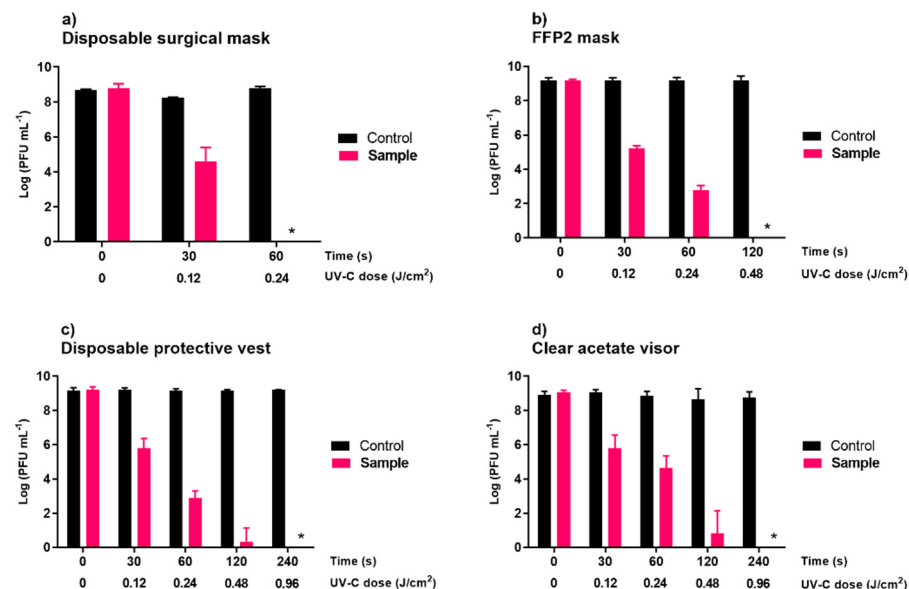


Figure 4. Inactivation of phage $\phi 6$ by the UV-C sterilizing chamber (8)5.5W on disposable surgical (a) and FFP2 (b) masks, disposable protective vest (c), and clear acetate visor (d). Limit of detection was about 2.3 log PFU/mL. Values represent the mean of the three experiments and error bars represent the standard deviation. * below the methods' detection limit.

When the surgical masks were disinfected with the UV-C light disinfection system, a reduction of approximately 8.8 log PFU/mL (ANOVA, $p < 0.05$, Figure 4a) was observed after 60 s of irradiation, reaching the detection limit of the method. However, after 30 s of irradiation, the viral inactivation was already high (4.2 log PFU/mL).

In the FFP2 masks, a reduction of approximately 9.2 log PFU/mL (ANOVA, $p < 0.05$, Figure 4b) was observed after 120 s of irradiation, reaching the detection limit of the method. However, after 30 and 60 s of irradiation, the viral inactivation was already 4.0 and 6.4 log PFU/mL (ANOVA, $p < 0.05$, Figure 4b), respectively.

In the clear acetate visor and disposable protective vests, the detection limit of the method (with a 9.2 log PFU/mL reduction) was only reached after 240 s. After 30, 120, and 180 s of irradiation, the viral inactivation for clear acetate visor and disposable vests was similar (ANOVA, $p > 0.05$). However, after 60 s of irradiation, the viral inactivation for the disposable vest (decrease 6.3 log PFU/mL) was higher than that observed for the clear acetate visor (decrease 4.5 log PFU/mL).

4. Discussion

Some reports affirmed that the SARS-CoV-2 virus can remain on different surfaces for variable periods while maintaining its infective potential [5,6,18]. These studies highlight the potential importance of surface contamination for the dissemination of SARS-CoV-2 in the population. This fact emphasizes the importance of proper surface disinfection and its impact on potential infections. Furthermore, there is still little evidence that UV light may be effective for inactivating SARS-CoV-2 [7,32]. In this study, the results showed that the UV-C light was effective in inactivating phage $\phi 6$. It is important to note that the viral concentration used in this study was higher than reported by Kampf et al. (2020) in naturally contaminated surfaces. According to these authors, the SARS-CoV-2 concentrations per swab were 4.4–5.2 log₁₀ in intensive care units and 2.8–4.0 log₁₀ in general wards [9]. This demonstrates that UV-C systems can be effective against viral concentrations higher than those reported in the literature corresponding to naturally contaminated surfaces.

Hygiene practices for surfaces have led to several modifications in human habits and the development of innovative and efficient cleaning procedures [7]. In addition to chemicals, physical disinfection methods can be fast and less time-consuming thanks to the possibility of being carried out by automated instruments and applied on solid surfaces and aerosols [17]. In this study, both of the new UV-C systems reduced phage $\phi 6$ concentration in magnitudes, depending on the irradiance power between the UV-C systems and the UV dosage within the UV-C systems (Figures 2 and 3). As the disinfection time increased, the effective reduction of phage $\phi 6$ of both systems increased. The results showed that the UV-C sterilizing chamber (8)5.5W (irradiance of 4.0 mW/cm²) system inactivated the phage $\phi 6$ faster than the UV-C sterilizing chamber (2)2.4W (irradiance of 1.0–2.5 mW/cm²) (Figures 2 and 3). For the inanimate surfaces, the UV-C sterilizing chamber (8)5.5W was able to inactivate phage $\phi 6$ below the detection limit of the method after 30–60 s of irradiation (UV-C doses of 0.12–0.24 J/cm²) (Figure 3). In the UV-C sterilizing chamber (2)2.4W, the maximum viral inactivation was 4.1, 4.2, 6.3, and 6.2 log PFU/mL in plastic, glass, stainless steel, and wood, respectively, achieved after 120 s of irradiation (UV-C dose of 0.3 J/cm²) (Figure 2). Based on our results, UV-C irradiation of 4.0 mW/cm² applied for 60 s (giving a UV-C dose of 0.24 J/cm²) is enough to reduce the viral titer below the detection limit of the method. Tseng and Li (2007) observed that a UV dose of 3.80 to 5.36 mJ/cm² was required to efficiently reduce phage $\phi 6$ titer (90%) [51]. According to some studies, single-stranded nucleic acid viruses (such as SARS-CoV-2) are more susceptible to UV inactivation on surfaces than double-stranded nucleic acid viruses (such as phage $\phi 6$) [51,52]. Ma et al. (2021) evaluated the efficiency of five UV-C devices in the inactivation of three enveloped viruses (two coronaviruses, HCoV 229E and MHV; and phage $\phi 6$) and observed that phage $\phi 6$ was more resistant to UV radiation damage than the two coronaviruses [52]. In addition, phages are more resistant to UV-C radiation than other pathogenic viruses in the environment [51]. The shorter genome size of phages, compared to the animal viruses, leads to its higher UV resistance [23,53]. The nucleic acid sequence composition in the genome also affects the viral UV irradiation sensitivity in which adjacent pyrimidines are photoreactive under UV-C irradiation, forming pyrimidine dimers [1,18,19,52]. Thus, fewer adjacent pyrimidines in a phage's genome may also contribute to its higher UV resistance.

So, inactivation methods that are effective against phage $\phi 6$ will be also effective against the SARS-CoV-2. Therefore, viruses such as SARS-CoV-2 may be more susceptible to UV-C inactivation than the phage used in this study. However, further studies using different viruses and different viral concentrations are necessary to validate these results. It should be highlighted that only one phage was studied and the current results need to be further validated for other viruses, including the SARS-CoV-2.

The effectiveness of UV-C light also depends on the type of surface on which it is applied [18]. In the UV-C sterilizing chamber (2)2.4W, the maximum viral inactivation was 4.1, 4.2, 6.3, and 6.2 log PFU/mL in plastic, glass, stainless steel, and wood, respectively, achieved after 120 s of irradiation (UV-C dose of 0.3 J/cm²). The UV-C sterilizing chamber (8)5.5W was able to inactivate phage $\phi 6$ below the detection limit of the method after only 30 s in glass (UV-C dose of 0.12 J/cm²) and 60 s (UV-C dose of 0.24 J/cm²) in plastic, stainless steel, and wood. However, the viral concentration decreased by approximately 3.6, 5.0, and 3.7 log PFU/mL in plastic, stainless steel, and wood after 30 s of irradiation. Similar results were obtained by Gidari et al. (2021). These authors observed that plastic and stainless steel surfaces needed higher UV-C doses to achieve the target reduction [7]. The total inactivation of SARS-CoV-2 on glass was obtained with the lowest dose applied. Uneven and porous surfaces are considered problematic due to the lack of UV-C light penetration. UV-C light does not readily penetrate solid surfaces as light is absorbed or reflected by the substrate material. Decontamination efficacy decreases if the UV-C light cannot effectively penetrate shielded areas [51]. According to certain authors, plastic seems to be the most UV-C refractory material, followed by stainless steel and glass [7].

Due to the increased demand for PPE as a result of the current SARS-CoV-2 pandemic, decontamination and reuse of disposable surgical and FFP2 masks, disposable protective vests, and clear acetate visors may be required to ensure continued availability. Córdoba-Lánus et al. (2021) observed that PPE materials (gowns and masks) infected with a SARS-CoV-2 positive clinical sample retained their infectivity up to 5–7 days post-infection [54]. In another study, the authors observed that the SARS-CoV-2 maintained its infectiveness for 7 days post-infection in surgical masks [5]. Our results showed a reduction of approximately 8.8 and 9.2 log PFU/mL in disposable surgical and FFP2 masks, reaching the detection limit of the method, after 60 (UV-C dose of 0.24 J/cm²) and 120 s (UV-C dose of 0.48 J/cm²) of irradiation, respectively. The FFP2 masks contain multiple layers of filtration and breathing droplets may penetrate the inner layers. Fisher et al. (2011) demonstrated that the UV-C light was able to penetrate FFP masks, however, light transmittance ranges from 23–50% through the outer layer, depending on the FFP mask model [55]. In the clear acetate visor and disposable protective vests, the detection limit of the method (with a 9.1 log PFU/mL reduction) was only reached after 240 s (UV-C dose of 0.96 J/cm²). The ability of UV-C light to thoroughly sanitize PPE may vary based on its ability to penetrate the material.

In the future, it will be essential to understand the efficacy of UV-C light on SARS-CoV-2 using different viral concentrations, environmental conditions, and materials. Bianco et al. (2020) demonstrated that viral inhibition varied as a function of UV-C intensity and viral concentration [56]. Some studies have also shown that viral stability seems to be influenced by the characteristics of the different materials but also by environmental conditions such as temperature, pH, and humidity [5,12–14]. However, these factors were not considered in the current study.

5. Conclusions

UV-C irradiation can provide efficient, rapid, and sustainable sanitization procedures for different surfaces and PPE. Both UV-C systems were effective in inactivating phage $\phi 6$, but that effectiveness was material-dependent. Plastic, stainless steel, and wood surfaces (60 s) needed more time to achieve the viral inactivation to the detection limit of the method when compared with glass (30 s). For the disposable surgical masks and FFP2 masks, the viral inactivation was also more effective (60 and 120 s, respectively, to reach the detection

limit of the method) than the inactivation in clear acetate visors and disposable protective vests (240 s to reach the detection limit of the method). Irradiance and irradiation period are important parameters to consider in the implementation of this technology as an important approach to fight the SARS-CoV-2 pandemic. Further studies are needed to validate these findings using SARS-CoV-2 at different concentrations, in different environmental conditions, and in different materials.

Author Contributions: M.B. (Maria Bartolomeu), M.B. (Márcia Braz), P.C. and J.D. performed the experiments. C.P., M.B. (Maria Bartolomeu), M.B. (Márcia Braz), P.C. and J.D. participated in the conception and design of the experiments, and analysis of the resulting data. C.P. wrote the paper and M.B. (Maria Bartolomeu), M.B. (Márcia Braz), P.C. and J.D. also contributed to the writing. A.A. supervised the work, revised the paper, and contributed with reagents and analysis tools. All authors have read and agreed to the published version of the manuscript.

Funding: We acknowledge financial support to CESAM by FCT/MCTES (UIDP/50017/2020+UIDB/50017/2020+ LA/P/0094/2020), through national funds.

Institutional Review Board Statement: Not applicable.

Informed Consent Statement: Not applicable.

Data Availability Statement: Not applicable.

Acknowledgments: Thanks are also due to the Department of Biology and University of Aveiro where this research was carried out. The authors are also grateful to CESAM and its funding sources. Maria Bartolomeu, Pedro Costa, Márcia Braz, and João Duarte thank the Portuguese Foundation for Science and Technology (FCT) for their doctoral grant (SFRH/BD/121645/2016, PD/BD/150360/2019; 2020.06571.BD, and 2021.05519.BD, respectively). Carla Pereira acknowledges the FCT for Junior Research contract (CEEC Individual/03974/2017). We thank Angélica Lopes for the graphical design of the UV-C light disinfection systems.

Conflicts of Interest: The authors declare no conflict of interest.

References

1. Raeiszadeh, M.; Adeli, B. A Critical review on ultraviolet disinfection systems against COVID-19 outbreak: Applicability, validation, and safety considerations. *ACS Photonics* **2020**, *7*, 2941–2951. [[CrossRef](#)]
2. Subbarao, K.; Mahanty, S. Respiratory virus infections: Understanding COVID-19. *Immunity* **2020**, *52*, 905–909. [[CrossRef](#)] [[PubMed](#)]
3. WHO. Coronavirus Disease (COVID-19): How Is It Transmitted? Available online: <https://www.who.int/news-room/questions-and-answers/item/coronavirus-disease-covid-19-how-is-it-transmitted> (accessed on 12 February 2022).
4. Otter, J.A.; Donskey, C.; Yezli, S.; Douthwaite, S.; Goldenberg, S.D.; Weber, D.J. Transmission of SARS and MERS coronaviruses and influenza virus in healthcare settings: The possible role of dry surface contamination. *J. Hosp. Infect.* **2016**, *92*, 235–250. [[CrossRef](#)] [[PubMed](#)]
5. Chin, A.; Chu, J.; Perera, M.; Hui, K.; Yen, H.-L.; Chan, M.; Peiris, M.; Poon, L. Stability of SARS-CoV-2 in different environmental conditions. *Lancet Microbe* **2020**, *1*, e10. [[CrossRef](#)]
6. Doremalen, N.; Bushmaker, T.; Morris, D.; Holbrook, M.; Gamble, A.; Williamson, B.; Tamin, A.; Harcourt, J.; Thornburg, N.; Gerber, S.; et al. Aerosol and surface stability of SARS-CoV-2 as compared with SARS-CoV-1. *N. Engl. J. Med.* **2010**, *382*, 1564–1567. [[CrossRef](#)]
7. Gidari, A.; Sabbatini, S.; Bastianelli, S.; Pierucci, S.; Busti, C.; Bartolini, D.; Stabile, A.M.; Monari, C.; Galli, F.; Rende, M.; et al. SARS-CoV-2 survival on surfaces and the effect of UV-C light. *Viruses* **2021**, *13*, 408. [[CrossRef](#)]
8. Gonçalves, J.; Da Silva, P.; Reis, L.; Nascimento, M.; Koritnik, T.; Paragi, M.; Mesquita, J. Surface contamination with SARS-CoV-2: A systematic review. *Sci. Total Environ.* **2021**, *798*, 149231. [[CrossRef](#)]
9. Kampf, G.; Todt, D.; Pfaender, S.; Steinmann, E. Persistence of coronaviruses on inanimate surfaces and their inactivation with biocidal agents. *J. Hosp. Infect.* **2020**, *104*, 19–21. [[CrossRef](#)]
10. Kaba, H.E.J.; Steinmann, J.; Pfaender, S.; Kampf, G.; Bru, Y.; Scheithauer, S.; Steinmann, E. Potential sources, modes of transmission and effectiveness of prevention measures against SARS-CoV-2. *J. Hosp. Infect.* **2020**, *106*, 678–697. [[CrossRef](#)]
11. Lv, J.; Yang, J.; Xue, J.; Zhu, P.; Liu, L.; Li, S. Detection of SARS-CoV-2 RNA residue on object surfaces in nucleic acid testing laboratory using droplet digital PCR. *Sci. Total Environ.* **2020**, *742*, 140370. [[CrossRef](#)]
12. Riddell, S.; Goldie, S.; Hill, A.; Eagles, D.; Drew, T.W. The effect of temperature on persistence of SARS-CoV-2 on common surfaces. *Virology* **2020**, *17*, 145. [[CrossRef](#)] [[PubMed](#)]

13. Magurano, F.; Baggieri, M.; Marchi, A.; Rezza, G.; Nicoletti, L.; Eleonora, B.; Concetta, F.; Stefano, F.; Maedeh, K.; Paola, B.; et al. SARS-CoV-2 infection: The environmental endurance of the virus can be influenced by the increase of temperature. *Clin. Microbiol. Infect.* **2021**, *27*, 289.e5–289.e7. [[CrossRef](#)] [[PubMed](#)]
14. Biryukov, J.; Boydston, J.A.; Dunning, R.A.; Yeager, J.J.; Wood, S.; Reese, A.L.; Ferris, A.; Miller, D.; Weaver, W.; Zeitouni, N.E.; et al. Increasing temperature and relative humidity accelerates inactivation of SARS-CoV-2 on surfaces. *mSphere* **2020**, *5*, e00441-20. [[CrossRef](#)] [[PubMed](#)]
15. Kumar, S.; Singh, R.; Kumari, N.; Karmakar, S.; Behera, M.; Siddiqui, A.J. Current understanding of the influence of environmental factors on SARS-CoV-2 transmission, persistence, and infectivity. *Environ. Sci. Pollut. Res.* **2021**, *28*, 6267–6288. [[CrossRef](#)]
16. Heßling, M.; Hönes, K.; Vatter, P.; Lingenfelder, C. Ultraviolet irradiation doses for coronavirus inactivation—Review and analysis of coronavirus photoinactivation studies. *GMS Hyg. Infect. Control* **2020**, *15*, Doc08. [[CrossRef](#)] [[PubMed](#)]
17. Beggs, C.B.; Avital, E.J. Upper-room ultraviolet air disinfection might help to reduce COVID-19 transmission in buildings: A feasibility study. *PeerJ* **2020**, *8*, e10196. [[CrossRef](#)]
18. Hadi, J.; Dunowska, M.; Wu, S.; Brightwell, G. Control measures for SARS-V-2: A review on light-based inactivation of single-stranded rna viruses. *Pathogens* **2020**, *9*, 737. [[CrossRef](#)]
19. Cutler, T.; Zimmerman, J. Ultraviolet irradiation and the mechanisms underlying its inactivation of infectious agents. *Anim. Health Res. Rev.* **2011**, *12*, 15–23. [[CrossRef](#)]
20. Wurtmann, E.J.; Wolin, S.L. RNA under attack: Cellular handling of RNA damage. *Crit. Rev. Biochem. Mol. Biol.* **2009**, *44*, 34–49. [[CrossRef](#)]
21. Wigginton, K.R.; Menin, L.; Sigstam, T.; Gannon, G.; Cascella, M.; Hamidane, H.B.; Tsybin, Y.O.; Waridel, P.; Kohn, T. UV radiation induces genome-mediated, site-specific cleavage in viral proteins. *ChemBioChem* **2012**, *13*, 837–845. [[CrossRef](#)]
22. Reed, N.G. The history of ultraviolet germicidal irradiation for air disinfection. *Public Health Rep.* **2010**, *125*, 15–27. [[CrossRef](#)] [[PubMed](#)]
23. Kowalski, W.J.; Bahnfleth, W.P.; Hernandez, M.T. A genomic model for predicting the ultraviolet susceptibility of viruses and bacteria. In Proceedings of the IUVA Conference, Amsterdam, The Netherlands, 21–25 September 2009; Volume 11, pp. 15–28.
24. Mojica, K.D.A.; Brussaard, C.P.D. Factors affecting virus dynamics and microbial host-virus interactions in marine environments. *FEMS Microbiol. Ecol.* **2014**, *89*, 495–515. [[CrossRef](#)] [[PubMed](#)]
25. Lytle, C.D.; Sagripanti, J.-L. Predicted inactivation of viruses of relevance to biodefense by solar radiation. *J. Virol.* **2005**, *79*, 14244–14252. [[CrossRef](#)] [[PubMed](#)]
26. Perlmutter, J.; Hagan, M. Mechanisms of virus assembly. *Annu. Rev. Phys. Chem.* **2015**, *66*, 217. [[CrossRef](#)] [[PubMed](#)]
27. Meo, S.A.; Alhowikan, A.M.; Khlawi, T.A.L.; Meo, I.M.; Halepoto, D.M.; Iqbal, M.; Usmani, A.M.; Hajjar, W.; Ahmed, N. Novel coronavirus 2019-nCoV: Prevalence, biological and clinical characteristics comparison with SARS-CoV and MERS-CoV. *Eur. Rev. Med. Pharmacol. Sci.* **2020**, *24*, 2012–2019. [[CrossRef](#)] [[PubMed](#)]
28. Pinon, A.; Vialette, M. Survival of viruses in water. *Intervirology* **2019**, *61*, 214–222. [[CrossRef](#)]
29. Santos, A.L.; Moreirinha, C.; Lopes, D.; Esteves, A.C.; Henriques, I.; Almeida, A.; Domingues, M.R.M.; Delgadillo, I.; Correia, A.; Cunha, A. Effects of UV radiation on the lipids and proteins of bacteria studied by mid-infrared spectroscopy. *Environ. Sci. Technol.* **2013**, *47*, 6306–6315. [[CrossRef](#)]
30. Sabino, C.P.; Sellera, F.P.; Sales-Medina, D.F.; Machado, R.R.G.; Durigon, E.L.; Freitas-Junior, L.H.; Ribeiro, M.S. UV-C (254 nm) lethal doses for SARS-CoV-2. *Photodiagn. Photodyn. Ther.* **2020**, *32*, 101995. [[CrossRef](#)]
31. Inagaki, H.; Saito, A.; Sugiyama, H.; Okabayashi, T.; Fujimoto, S. Rapid inactivation of SARS-CoV-2 with Deep-UV LED irradiation. *Emerg. Microbes Infect.* **2020**, *9*, 1744–1747. [[CrossRef](#)]
32. Heilingloh, C.S.; Aufderhorst, U.W.; Schipper, L.; Dittmer, U.; Witzke, O.; Yang, D.; Zheng, X.; Sutter, K.; Trilling, M.; Alt, M.; et al. Susceptibility of SARS-CoV-2 to UV irradiation. *Am. J. Infect. Control* **2020**, *48*, 1273–1275. [[CrossRef](#)]
33. Ozog, D.M.; Sexton, J.Z.; Narla, S.; Pretto-Kernahan, C.D.; Mirabelli, C.; Lim, H.W.; Hamzavi, I.H.; Tibbetts, R.J.; Mi, Q.S. The effect of ultraviolet C radiation against different N95 respirators inoculated with SARS-CoV-2. *Int. J. Infect. Dis.* **2020**, *100*, 224–229. [[CrossRef](#)] [[PubMed](#)]
34. Fischer, C.R.; Yoichi, M.; Unno, H.; Tanji, Y. The coexistence of *Escherichia coli* serotype O157:H7 and its specific bacteriophage in continuous culture. *FEMS Microbiol. Lett.* **2004**, *241*, 171–177. [[CrossRef](#)] [[PubMed](#)]
35. Boyce, J.; Donskey, C. Understanding ultraviolet light surface decontamination in hospital rooms: A primer. *Infect. Control Hosp. Epidemiol.* **2019**, *40*, 1030–1035. [[CrossRef](#)] [[PubMed](#)]
36. Donskey, C.J. Decontamination devices in health care facilities: Practical issues and emerging applications. *Am. J. Infect. Control* **2019**, *47*, A23–A28. [[CrossRef](#)] [[PubMed](#)]
37. Casanova, L.; Weaver, S. Evaluation of eluents for the recovery of an enveloped virus from hands by whole-hand sampling. *J. Appl. Microbiol.* **2015**, *118*, 1210–1216. [[CrossRef](#)]
38. Whitworth, C.; Mu, Y.; Houston, H.; Martinez-Smith, M.; Noble-Wang, J.; Coulliette-Salmond, A.; Rose, L. Persistence of bacteriophage phi 6 on porous and nonporous surfaces and the potential for its use as an ebola virus or coronavirus surrogate. *Appl. Environ. Microbiol.* **2020**, *86*, e01482-20. [[CrossRef](#)]
39. Silverman, A.I.; Boehm, A.B. Systematic review and meta-analysis of the persistence and disinfection of human coronaviruses and their viral surrogates in water and wastewater. *Environ. Sci. Technol. Lett.* **2020**, *7*, 544–553. [[CrossRef](#)]

40. Vejerano, E.P.; Marr, L.C. Physico-chemical characteristics of evaporating respiratory fluid droplets. *J. R. Soc. Interface* **2018**, *15*, 20170939. [[CrossRef](#)]
41. Prussin, A.J.; Schwake, D.O.; Lin, K.; Gallagher, D.L.; Buttlng, L.; Marr, L.C. Survival of the enveloped virus phi6 in droplets as a function of relative humidity, absolute humidity, and temperature. *Appl. Environ. Microbiol.* **2018**, *84*, e00551-18. [[CrossRef](#)]
42. Turgeon, N.; Toulouse, M.-J.; Martel, B.; Moineau, S.; Duchaine, C. Comparison of five bacteriophages as models for viral aerosol studies. *Appl. Environ. Microbiol.* **2014**, *80*, 4242–4250. [[CrossRef](#)]
43. De Carvalho, N.A.; Stachler, E.N.; Cimabue, N.; Bibby, K. Evaluation of phi6 persistence and suitability as an enveloped virus surrogate. *Environ. Sci. Technol.* **2017**, *51*, 8692–8700. [[CrossRef](#)] [[PubMed](#)]
44. Fedorenko, A.; Grinberg, M.; Orevi, T.; Kashtan, N. Survival of the enveloped bacteriophage phi6 (a surrogate for SARS-CoV-2) in evaporated saliva microdroplets deposited on glass surfaces. *Sci. Rep.* **2020**, *10*, 22419. [[CrossRef](#)] [[PubMed](#)]
45. Rastogi, M.; Pandey, N.; Shukla, A.; Singh, S.K. SARS coronavirus 2: From genome to infectome. *Respir. Res.* **2020**, *21*, 318. [[CrossRef](#)] [[PubMed](#)]
46. Mindich, L. Precise packaging of the three genomic segments of the double-stranded-RNA bacteriophage phi6. *Microbiol. Mol. Biol. Rev.* **1999**, *63*, 149–160. [[CrossRef](#)] [[PubMed](#)]
47. Pinheiro, L.; Pereira, C.; Frazão, C.; Balcão, V.; Almeida, A. Efficiency of phage phi6 for biocontrol of *Pseudomonas syringae* pv. *syringae*: An in vitro preliminary study. *Microorganisms* **2019**, *7*, 1319–1330. [[CrossRef](#)]
48. Callanan, J.; Stockdale, S.R.; Shkoporov, A.; Draper, L.A.; Ross, R.P.; Hill, C. RNA phage biology in a metagenomic era. *Viruses* **2018**, *10*, 386. [[CrossRef](#)]
49. Mäntynen, S.; Sundberg, L.R.; Poranen, M.M. Recognition of six additional cystoviruses: *Pseudomonas* virus phi6 is no longer the sole species of the family *Cystoviridae*. *Arch. Virol.* **2018**, *163*, 1117–1124. [[CrossRef](#)]
50. Adams, M.H. *Bacteriophages*; Interscience Publishers, John Wiley and Sons Inc.: New York, NY, USA, 1959.
51. Tseng, C.C.; Li, C.S. Inactivation of viruses on surfaces by ultraviolet germicidal irradiation. *J. Occup. Environ. Hyg.* **2007**, *4*, 400–405. [[CrossRef](#)]
52. Ma, B.; Linden, Y.S.; Gundy, P.M.; Gerba, C.P.; Sobsey, M.D.; Linden, K.G. Inactivation of coronaviruses and phage phi6 from irradiation across UVC wavelengths. *Environ. Sci. Technol. Lett.* **2021**, *8*, 425–430. [[CrossRef](#)]
53. Rodriguez, R.A.; Bounty, S.; Beck, S.; Chan, C.; McGuire, C.; Linden, K.G. Photoreactivation of bacteriophages after UV disinfection: Role of genome structure and impacts of UV source. *Water Res.* **2014**, *55*, 143–149. [[CrossRef](#)]
54. Córdoba-Lanús, E.; García-Pérez, O.; Cazorla-Rivero, S.; Rodríguez-Esparragón, F.; Piñero, J.E.; Clavo, B.; Lorenzo-Morales, J. Persistence of SARS-CoV-2 infection on personal protective equipment (PPE). *BMC Infect. Dis.* **2021**, *21*, 1169. [[CrossRef](#)] [[PubMed](#)]
55. Fisher, E.M.; Shaffer, R.E. A method to determine the available UV-C dose for the decontamination of filtering facepiece respirators. *J. Appl. Microbiol.* **2011**, *110*, 287–295. [[CrossRef](#)] [[PubMed](#)]
56. Biasin, M.; Bianco, A.; Pareschi, G.; Cavalleri, A.; Cavatorta, C.; Fenizia, C.; Galli, P.; Lessio, L.; Lualdi, M.; Tombetti, E.; et al. UV-C irradiation is highly effective in inactivating SARS-CoV-2 replication. *Sci. Rep.* **2021**, *11*, 6260. [[CrossRef](#)] [[PubMed](#)]